Pergamon

0021-8928(95)00074-7

J. Appl. Maths Mechs, Vol. 59, No. 4, pp. 635–643, 1995

0021-8928/95 $24.00+0.00

ESTIMATES OF THE PRESSURES, TEMPERATURES AND DRAG COEFFICIENT IN THE SUPERSONIC FLOW OF A MEDIUM AROUND BLUNT BODIES†

I. V. SIMONOV

Moscow

(*Received* 28 *April* 1994)

Equations for determining the density, pressure and temperature at the stagnation point of steady supersonic flow around a body are obtained from the conservation laws on the leading shock wave front and the Bernoulli integral behind the front. Different relations defining the medium are used: in the form of the Mie–Grüneisen equation (soils and metals) and the Tate equation (fluids). An upper and lower estimate of the head drag is given on the basis of an hypothesis that the contact pressure field is equalized as the flow velocity increases, which is substantiated by well-known calculations. The results of calculations for two types of sands, clay and water are presented. The corrections, when account is taken of heat conduction, viscosity and plasticity, are found.

Certain geological media are distinguished by comparatively low values of the velocity of sound (several hundreds of metres in sands, loesses and firn). Hence, supersonic conditions for the motion of a research probe, and the need associated with this to estimate the pressure and temperature, can arise, for example, when investigating the physicomechanical properties of such structures on the surfaces of planets by dynamic penetration experiments.

It has been shown, when processing experimental data [1], that the hydrodynamic part of the drag force accompanying the subsonic motion of a body in a solid medium is described like that in a fluid of corresponding density. The forces which depend on solidity stabilize and become small at transonic velocities. A similar conclusion can be drawn from an asymptotic analysis of the problem of the elasto-plastic flow around slender bodies [2]. Simplified models of the supersonic motions of minimal drag bodies [3, 4], based on the well-known Lavrent'yev hypothesis concerning the similarity of the stress and velocity fields in a fluid and in a solid medium, contain a priori ideas regarding the effect of the compressibility of the medium and require calibration. Furthermore, from the point of view of the strength of the body around which the flow occurs, it is important to know the maximum pressure and temperature on its surface. The determination of these quantities is the principal aim of this paper.

Without recourse to the solution of the complex problem of the flow of a dense medium around a rigid body as a whole, comparatively simple equations and quadratures are obtained by analytic methods for calculating the pressure, density and temperature on the leading wave front and at the stagnation point of a flow. The medium is described by the Mie–Grüneisen equation of state and the linear law that the velocity of the wave is the velocity of the particles behind the front [5–10] or by the Tate equation [11]. The accuracy of the approximation corresponds to the actual accuracy of the experimental data with respect to the shock wave adiabatic curves and the thermodynamic parameters. Calculations were carried out for geological media (sands, clay and water) over a range of flow velocities from 0.5 to 4 km/s and pressures of up to ~10 GPa, that is, until the striker, made of high tensile materials, is obviously destroyed. As it turned out, the pressure increment outside the shock wave front predominates over the amplitude increment of this shock wave at low Mach numbers ($M = 2$), but, when $2 < M < 4$, the orders of both increments are the same. The temperature surges were found to be small compared with the melting points of refractory alloys and, obviously, due to the short duration of the process only have a small effect on the strength of the striker. It is important that the quantities found should be stable with respect to variations in the parameters of the medium. For instance, the pressure coefficients at a velocity of less than 3 km/s do not exceed a value of 1.4 in all cases. Estimates of the drag as well as estimates of the effect of viscosity, heat conduction and plasticity, that is, of factors which are not taken into account in the main context, are put forward. There are no experimental data for the velocity range indicated above, and a numerical experiment has only been carried out for water [12–14]. Similar

†*Prikl. Mat. Mekh.* Vol. 59, No. 4, pp. 662–671, 1995.

elements are contained in the theoretical papers [15, 16]. For instance, the most important of these in [16] is the assumption of the cavitational nature of the flow. Problems of thermodynamics are, however, not touched upon in [15, 16]. Hence, the results obtained in the present paper, while incomplete, provide new and important information concerning the characteristics of the flow and can be used for checking numerical algorithms.

Generally speaking, the possibility of cavitating flow follows immediately from Lavrent'yev's well-known hypothesis concerning the similarity of the characteristics of high-velocity flow in a fluid and in a solid medium. Specifically, cavitating flow around a body in a solid medium was apparently mentioned for the first time in a presentation of classified papers by English investigators during the war years [17] and, also, in [1, 3, 4].

1. PHYSICAL PREMISES

We consider the steady boundless supersonic flow of a condensed, inviscid and non-heat-conducting medium around an axially symmetric, blunt and absolutely rigid body. Flow separation conditions are studied. For simplicity, we shall assume that the separation line is specified by the configuration of the contour around which the flow occurs with a break (disk, segment, paraboloid, etc.). In view of the high pressure level, we neglect rigidity effects.

Under steady supersonic flow conditions $M = U_-/D_0 > 1$, where U_- and D_0 are the velocities of the free stream and the weak shock wave in the medium, respectively, a strong frontal shock wave $A'AA''$ (Fig. 1) is formed. The flow is unperturbed ahead of the front of this wave:

$$U = U_-, \quad P = 0, \quad T = T_-, \quad V = V_-, \quad E = 0 \tag{1.1}$$

where U is the mass velocity, P is the pressure, T is the temperature, and V and E are the specific volume and the specific internal energy. The parameters change abruptly on crossing the front (the corresponding values will be marked by a subscript plus) and continuously behind the front. (The values at the stagnation point B will be marked by an asterisk.) In order to describe the state of the solid, we adopt the well-known Mie–Grüneisen equation and the Tate equation in the case of water.

In a porous medium and for a comparatively small shock-wave amplitude, there is an irreversible bulk deformation of the medium in the case of loading behind the front, and, consequently, the assumption of isentropicity, which considerably simplifies the analysis, loses its meaning. In this case and in the absence of the requisite experimental data concerning the mechanical behaviour of a porous medium under high pressure and high temperature, we shall give an upper and a lower estimate of the required quantities, starting from the assumption that the loading process is either adiabatic or isentropic.

It can be shown that, at least at moderate values of the Mach number, the shock wave is located from the nose part of the body (compared with its transverse dimension). This means that the transition $A \Rightarrow B$ occurs with a considerable variation in the required functions and cannot be approximated using the simplest schemes (Newton's method, for example). Hence, we relate the states at the point of symmetry on the wave front A and at the stagnation point B using the Bernoulli integral for a compressible fluid subject to the condition for stagnation of the flow $U_* = 0$

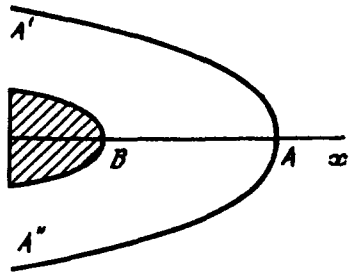

Fig. 1.

$$P_*U_* - P_+V_+ - \frac{U_+^2}{2} + V_- \int_{\theta_+}^{\theta_*} P_s(\theta)d\theta = 0, \quad \theta = 1 - \frac{V}{V_-} \tag{1.2}$$

Certain constraints, associated with the applicability of integral (1.2) are discussed in Section 7. We also write down the general conservation laws in the shock wave taking account of (1.1)

$$P_+ = U_-(U_- - U_+)/V_- = U_+(U_- - U_+)/V_+, \quad E_+ = P_+(V_- - V_+)/2 \tag{1.3}$$

When $M \leqslant 1$, there is no shock wave (point A is removed to infinity upstream when $M \Rightarrow 1 + 0$) and the Bernoulli integral then relates the states at point B and at infinity.

Equalities (1.1)–(1.3) are then closed by a governing relation of the form $E = E(P, V)$.

2. THE MIE–GRÜNEISEN EQUATION

In order to describe the state of solids in the high-pressure and high-temperature region we adopt an equation in the form of the Mie–Grüneisen equation using the shock adiabatic curve $P_H = P_H(\theta, V_-)$ and the relation for determining the Grüneisen parameter [5]

$$\Gamma/V = \Gamma_0/V_0 = \Gamma_-/V_- \tag{2.1}$$

where V_0 and Γ_0 are the values of the parameters of the continuous phase under normal conditions and Γ_- is the effective value which is identical to the value of Γ_0 if $V_0 = V_-$ (there is no porosity). The equation then takes the form

$$E = E_H(\theta, V_-) + V_-(P - P_H)/\Gamma_-, \quad E_H(\theta, V_-) = \theta V_- P_H(\theta, V_-)/2 \tag{2.2}$$

On additionally invoking the thermodynamic equality $P_s = -(dE/dV)_s$, as is customary, we initially obtain the ordinary differential equation for the isentropic lines and, then, its solution with the initial condition of starting from the shock adiabatic curve

$$P_s = P_H(\theta, V_-) + \frac{\Gamma_-}{2}\int_{\theta_+}^{\theta}\left(1 - x\frac{\partial}{\partial x}\right)P_H(x, V_-)\,\exp[\Gamma_-(x-\theta)]dx \tag{2.3}$$

Below, we shall be guided by experimental shock adiabatic curves. For many media, these curves are approximated by a linear relation between the wave velocity D and the mass velocity u in the laboratory system of coordinates [5]

$$D = D_0 + \lambda u \Rightarrow P_H = D_0^2\theta/V_-(1 + \lambda\theta)^2 \tag{2.4}$$

With conditions (2.2), the isentropic equation (2.3) takes the form (2.5), and, when it is substituted into integral (1.2), we obtain an equation for the deformation $\theta_* = 1 - V_*/V$ at the stagnation point. We now present the final form of the system of relations for finding the required quantities P_*, V_* and the pressure coefficient C_P

$$P_* = P_s(\theta_*) = P_H(\theta, V_-) - \Gamma_-V_-^{-1}D_0^2I(\theta_*, \theta_+), \quad C_P = 2V_-U_-^{-2}P_*$$

$$\theta_*(2 - \theta_*)(1 - \lambda\theta_*)^{-2} - 2[1 + \Gamma_-(1 - \theta_*)]I(\theta_*, \theta_+) = M^2 \tag{2.5}$$

$$I = \int_{\theta_+}^{\theta_*} \exp[\Gamma_-(x-\theta)]\frac{\lambda x^2 dx}{(1-\lambda x)^2}$$

The temperature at the stagnation point is calculated by summing its increments on the front and along the isentropic curve. The discontinuity on the front is found by integrating an equation which is derived from the thermodynamic identity

$$dT/T = dS/c_V - \Gamma dV/V \tag{2.6}$$

where S is the entropy, c_v is the specific heat capacity at a constant volume, and the equation for the

entropy along the shock adiabatic curve [5] is

$$2TdS = (V_- - V)dP + PdV \tag{2.7}$$

The relation between the temperatures T_+ and T_* is found by integrating Eq. (2.6) when $dS = 0$. As a result, we obtain

$$T_+ = T_-\exp(\Gamma_-\theta_+) + D_0^2 c_V^{-1} I(\theta_+, 0), \qquad T_* = T_+\exp[\Gamma_-(\theta_* - \theta_+)] \tag{2.8}$$

A dense medium. As an example of a dense geological medium ($V_0 = V_-$) we shall consider clay with a moisture content $w = 4\%$ and with the parameters [6–8]

$$D_0 = 1600 \text{ m/s}, \quad \lambda = 1.47, \quad 1/V_- = 2.15 \times 10^3 \text{ kg/m}^3, \quad c_V = 980 \text{ J/kg K}, \quad \Gamma_0 = 0.9$$

The last two values have been corrected using the usual additive approach for calculating mixtures. The values of the required quantities, calculated using Eqs (2.4), (2.5) and (2.8) are shown in Table 1. The temperature increments $\Delta T_+ = T_+ - T_-$ and $\Delta T_* = T_* - T_-$ are indicated and pressures are shown in GPa. A comparative analysis is given below.

A porous medium. Dry sand is a porous geological medium with a relatively low velocity of propagation of perturbations D_0. Experimental data for the shock adiabatic curve of one type of sand (sand A) and the values of C_V and Γ_0 are presented in [7–9]

$$D_0 = 500 \text{ m/s}, \quad \lambda = 2.4, \quad 1/V_- = 1.66 \times 10^3 \text{ kg/m}^3, \quad 1/V_0 = 2.65 \times 10^3 \text{ kg/m}^3$$
$$c_V = 790 \text{ J/kg K}, \quad \Gamma_- = 1 \quad (692 < D < 2900 \text{ m/s}, \quad 1.4 < M < 5.8, \quad 0.1 < P_H < 5 \text{ GPa})$$

Breakdown of the sand particles and filling of the pores [9] occurs in the indicated range of amplitudes of the shock wave. A further loading and irreversible reduction in the porosity occur behind the front. This process cannot be considered as being isentropic. The construction of the exact equation for the process is made difficult by the lack of data on the compressibility of sand at high pressures, deformation rates and temperatures. We shall therefore confine ourselves to estimating the upper and lower limits of the required quantities.

Thus, the shock wave adiabatic curve (2.4) can be used as an equation for the process of rapid loading. Actually, the real discontinuity in the sand is spread out over a width of several characteristic dimensions of the microstructure, and, in the case when the body has relatively small transverse dimensions, it can be assumed that the shock loading continues along to point B, only in two stages. It then follows that one puts $I \equiv 0$ in the computational equation (2.5). The equation for θ_* becomes quadratic, and the required root is found using the formula

$$\theta_* = (1 + M^2 - \sqrt{1 + (2 - \lambda^{-1})M^2}) / (\lambda M^2 + 1)$$

The pressure P_* is found next using the equation of the shock adiabatic curve (2.4), and we shall calculate the temperature T_* using the first formula of (2.8), as is also done for T_+ having replaced θ_+ by θ_*. It is obvious here that the thermal part of the internal energy, the production of entropy and the temperature will be too high while we obtain a lower bound in the case of the mechanical characteristics P_*, $\rho_* = V_-/V_*$ (the relative density) and C_P. The opposite estimates are obtained by starting from the approximation of the isentropic curve (2.5)–(2.8). Note that the calculations give a very narrow range for the true values of the mechanical parameters while the width of the range for the temperature T_* increases considerably with the amplitude of the shock wave.

Numerical values of the quantities are shown in Table 1 where, when necessary, they are labelled with the subscripts i (an isentropic curve) and a (an adiabatic curve). The results for sand B, which is artificially prepared quartz crumb (the α-phase), are also presented there. The parameters of its shock adiabatic curve have been measured over a larger range of velocities and pressures [10]

$$D_0 = 1250 \text{ m/s}, \quad \lambda = 1.375, \quad 1/V_- = 1.75 \times 10^3 \text{ kg/m}^3, \quad 1/V_0 = 2.65 \times 10^3 \text{ kg/m}^3$$
$$c_V = 790 \text{ J/kg K}, \quad \Gamma_- = 1 \quad (2.1 < D < 4.14 \text{ km/s}, \quad 1.68 < M < 3.3, \quad 2.28 < P_H < 15.4 \text{ GPa})$$

The calculated "isentropic" and "adiabatic" values for both types of sand conform to the inequalities

$$\rho_{*\alpha} < \rho_{*i}, \quad P_{*\alpha} < P_{*i}, \quad C_{P\alpha} < C_{Pi}, \quad T_{*\alpha} > T_{*i}$$

The calculations show that the maximum pressures $P_{*\alpha}$ and P_{*i} are close in value. When $M < 5$, the relative difference did not exceed 11%. The temperature increments are not too different only for small shock wave amplitudes. It is natural to assume that the true values lie within the ranges and are initially closer to the "adiabatic" values, and must then approach the results of the calculation using the isentropic curve as the Mach number increases and the porosity on the wave front is depleted.

Table 1

M	ρ_+	ρ_{*i}	ρ_{*a}	P_+, GPa	P_{*i}, GPa	P_{*a}, GPa	ΔT_+, K	ΔT_{*a}, K	$\Delta T_{*}a$, K	C_{Pi}	C_{Pa}
					Sand *A*						
1.2	1.07	1.27	1.26	0.04	0.35	0.33	20	67	75	1.17	1.11
1.5	1.16	1.32	1.31	0.13	0.57	0.53	44	80	98	1.21	1.14
2	1.26	1.39	1.38	0.35	1.04	0.97	77	104	145	1.26	1.16
2.5	1.33	1.44	1.43	0.65	1.67	1.52	111	134	207	1.29	1.18
3	1.39	1.48	1.46	1.04	2.44	2.22	153	174	285	1.31	1.19
5	1.50	1.56	1.55	3.46	6.99	6.30	431	449	786	1.35	1.21
7	1.56	1.60		7.26	13.9		911	932		1.37	
					Sand *B*						
1.1	1.07	1.40	1.38	0.22	2.02	2.64	20	93	145	1.22	1.16
1.5	1.32	1.60	1.55	1.49	4.09	3.74	111	167	315	1.33	1.22
2	1.57	1.82	1.75	3.98	7.75	6.96	340	396	697	1.42	1.27
2.5	1.77	1.99	1.92	7.46	12.6	11.2	762	830	1303	1.47	1.32
					Clay						
1.1	1.07	1.37		0.41	4.04		12	57		1.21	
1.5	1.29	1.55		2.81	8.11		84	117		1.31	
2	1.52	1.73		7.49	15.3		315	349		1.39	
2.5	1.69	1.88		14.0	24.8		772	814		1.44	

Comparison of the results for the different types of sands and clay for the same flow velocity shows the closeness of the pressure values ($P_{*\alpha}$ = 6.3, 7.0 and 8.1 GPa when $U_- \cong 2.5$ km/s, respectively). Close temperature increments are only observed in the case of the sands. In the case of the clay, they are considerably smaller: T_{*i} = 732, 679 and 400 K. Note the low sensitivity of the calculated quantities to variation of the Grüneisen coefficient. For instance, an increase in the parameter Γ_0 by a factor of 1½ led to only a 10% increase in the temperature T_* (clay) while the values of P_* remained practically unchanged. This is important, since this coefficient is found indirectly from experiments and is of low accuracy.

The degenerate case of a porous medium ($D_0 = 0$). We know that, for a certain value of the porosity (~0.5 in the case of pliant metals [5]), the characteristic velocity D_0 vanishes and this degenerate case should be considered separately. When $D = U_- = \lambda u$, the relations on the front (2.4) and (2.8) take the form

$$\theta_+ = \frac{1}{\lambda}, \quad P_+ = \frac{\theta_+ U_-^2}{V_-} = \frac{U_-^2}{\lambda V_-}, \quad T_+ = \frac{U_-^2}{2\lambda^2 c_V} + T_-, \quad E_+ = \frac{U_-^2}{2\lambda^2}$$

The density is constant on the front and equal to the density of the continuous phase under normal conditions ($V_+ = V_0$). In other words, the so-called "snow plough" model is possible. By postulating that the loading process is isentropic and an equation of state for the continuous phase of the form (2.2) with a normal shock adiabatic curve $D = D_1 + \Lambda u$ and following the procedure similar to that described in Section 2, we obtain the equation of the isentropic curve behind the shock wave front and the equation for determining the deformation

$$P_s(\Theta) = P_H(\Theta, V_0) + P_+ \exp(\Gamma_0\Theta) - \Gamma_0 V_0^{-1} D_1^2 I(\Theta, 0)$$

$$P_* = P_s(\Theta_*), \quad T_* = T_+ \exp(\Gamma_0\Theta_*), \quad \frac{\Theta_*(2-\Theta_*)}{(1-\Lambda\Theta_*)^2} - 2\left(1+\Gamma_0\frac{V_*}{V_0}\right) I(\Theta_*, 0) =$$

$$= \frac{2(\Lambda-1)U_-^2}{\Lambda^2 D_1^2}\left\{\frac{\Lambda+1}{2} + \frac{1}{\Gamma_0} - \left(\frac{1}{\Gamma_0} + \frac{V_*}{V_0}\right)\exp(\Gamma_0\Theta_*)\right\}$$

At even higher values of the porosity, the magnitude of D_0 is negative, but then, if the linear law (2.2) remains true, the preceding treatment is also valid subject to the condition that $M < 0$.

3. THE TATE EQUATION

Since, above a certain value $P > 8$ GPa, the static and dynamic adiabatic curves for water start to differ, we shall use a corrected Tate equation to describe the motion of a body in water and the interpolation formula for the temperature jump [11]

$$P_H(\rho) = \frac{0.309(\rho^n - 1)}{1 + 0.7(\rho - 1)^4} \text{ GPa}, \quad \Delta T_H = 26.3\rho_H P_H(\rho_H), \quad \rho = \frac{V_-}{V} \tag{3.1}$$

It is more convenient to use the Tate equation without a correction term in the denominator for motions at Mach numbers $M < 2$. The calculation then reduces to solving the algebraic equation for the density in the shock wave and the subsequent calculation of the quantities at the stagnation point using the final formulae

$$nM^2(1-\rho_+^{-1}) = \rho_+^n - 1, \quad \frac{\rho_*}{\rho_+} = \left[1 + \frac{M^2(n-1)}{2\rho_+^{n+1}}\right]^{1/(n-1)}, \quad P_* = \frac{c_-^2}{nV_-}(\rho_*^n - 1)$$

$$n = 7.3, \quad c_- = 1500 \text{ m/s}, \quad V_- = 10^{-3} \text{ m}^3/\text{kg}$$

In calculations at $M > 1$ using the earlier algorithm (2.4)–(2.8), the parameters λ and Γ_0 were selected subject to the condition that P_+ and T_+ are identical with the values given by (3.1)

$$\lambda = 2, \quad \Gamma_0 = 0.7 \quad (0 < M < 2); \quad \lambda = 1.9;\ 1.8, \quad \Gamma_0 = 0.85 \quad (M = 2.5;\ 3)$$

while the heat capacity coefficient was estimated using the data in [11] as c_V = 3700 J/kg K. The results of the calculations are collected together in Table 2.

Table 2

M	ρ_+	ρ_*	P_+, GPa	P_*, GPa	ΔT_+, K	ΔT_*, K	C_P	C_{x0}/C_P	C_{xe}
0.5	1	1.10	0	0.30	0	–	1.05	0.86	1.02
1	1	1.26	0	1.33	0	–	1.15	0.95	1.1
1.5	1.20	1.39	0.84	3.14	41	69	1.24	1.02	
2	1.33	1.49	2.25	5.85	86	107	1.30	1.07	1.2
2.5	1.46	1.6	4.44	9.51	185	210	1.35	1.11	
3	1.59	1.72	7.50	14.2	324	349	1.40	1.15	1.25
3.5	1.73	1.85	11.6	19.9	539	568	1.44	1.18	

If one compares the numerical values for water with the data in Table 1, the following can be noted. As a consequence of the difference in the heat capacity of water and clay, there is also a pronounced difference in the temperature increments and, at the same flow velocities, they behave in approximately the same way as the coefficients c_V. Roughly speaking, the ratio of the pressures P_* is the same as the ratio of the initial densities, and the consolidation of ρ_* is also appreciably higher in the case of the clay.

4. ESTIMATES OF THE DRAG COEFFICIENT

The pressure coefficient C_P characterizes the effect of the compressibility of the medium and only changes slightly over the range of flow velocities considered: $1.135 < C_{P\alpha} < 1.214$, $1.5 < M < 5$ (sand A). In this case, the extrapolated values of C_P when $M = 1$ are equal to 0.153, 1.1, 1.15 and 1.2 for water, sand A, sand B and the clay, respectively, and, when $U_- < 3$ km/s, the value of C_P does not exceed 1.4 in all cases. It is important that this coefficient determines the upper limit of the coefficient of frontal drag C_x which is equal to the product of the drag and $2 \times V_-/U_-^2$. This assertion follows from the condition $P \leqslant P_*$ on a wetted surface. On the other hand, if the form of the distribution of the pressure P over this surface were to be invariant with respect to the Mach number, then $C_x = C_{x0}C_P$, where C_{x0} is the value of C_x when $M = 0$. However, as calculations of the flow of compressible water past cones have shown [12], this distribution levels off as the Mach number increases: $P \to P_*$, $C_x \to C_P - 0$. When $M = 2$–3, the coefficient C_P already gives a poor approximation of the upper value of C_x. We therefore conclude that

$$C_{x0}C_P < C_x < C_P \tag{4.1}$$

In the case of a disk $C_{x0} = 0.82$ [13], and the interval (4.1) is quite narrow. For instance, the arithmetic means from the ends of the interval (4.1) $\langle C_x \rangle = 1/2C_P(C_{x0} + 1)$ (Table 2) are identical with the results of a numerical experiment C_{xe} [13]. In the case of a sphere $C_{x0} = 0.44$ and (4.1) is a coarse estimate.

5. ESTIMATES OF THE EFFECT OF HEAT CONDUCTION, VISCOSITY AND PLASTICITY

In the case of a linearly viscous and heat conducting fluid, the equation for the change in the energy of the particles is described in the form [14]

$$\frac{DH}{Dt} = V\frac{\partial}{\partial x_i}(U_i\tau_{ij}) + kV\Delta T, \quad H = \frac{1}{2}U_i^2 + E + PV \tag{5.1}$$

$$\tau_{ij} = 2\eta\left(e_{ij} - \frac{1}{3}e\delta_{ij}\right), \quad e_{ij} = \frac{1}{2}\left(\frac{dU_i}{dx_j} + \frac{dU_j}{dx_i}\right), \quad e = e_{ii} \quad (i, j = 1,2,3)$$

where x_i is a Cartesian system of coordinates (x_1 = the x-axis), U_i are the components of the velocity vector, η is the coefficient of viscosity, τ_{ij} are the components of the viscous stress tensor and k is the thermal conductivity. From the symmetry conditions on the axis $r = (x_2^2 + x_3^2)^{1/2} = 0$ and the fact that there are no rotations about the axis, we obtain for the components which are not identically equal to zero

$$U_r = \partial U_r / \partial x = \partial U / \partial r = \tau_{rx} = 0, \quad r = 0, \quad U = U_1 \tag{5.2}$$

Next, using (5.2) and the equation of linear heat conduction with the heat capacity at constant pressure c_p, we reduce the energy conservation equation (5.1) for particles on the AB axis in a steady flow to the form

$$U\frac{\partial H}{\partial x} = \frac{4}{3}\eta V\left(\frac{\partial}{\partial x}U\frac{\partial U}{\partial x} + \left(\frac{\partial U}{\partial r}\right)^2\right) + Uc_P\frac{\partial T}{\partial x} \tag{5.3}$$

Equation (5.3) can serve as a basis for calculating the corrections to the zeroth approximation. Firstly, we shall study the effect of heat conduction separately. On integrating (5.3) along AB when $\eta = 0$ we obtain

$$H_* - H_+ = c_P(T_* - T_+) \tag{5.4}$$

The left-hand side of (5.4) is identical with the left-hand side of (1.2). On evaluating the temperature contribution using the perturbation method we arrive at the conclusion that the right-hand side of (5.4) (the perturbation) constitutes about 1% (several percent) of the most significant term of P_*V_* in the case of the clay (sands). This falls within the limits of the acceptable accuracy.

We shall now study the effect of viscosity, putting $k = 0$. With the aim of deriving an analytic estimate, we shall specify a certain real shape for the nose section of the body (a hemisphere of radius a) and assume that the velocity distribution along AB is not too different from the analogous distribution in a flow of an ideal incompressible fluid around a sphere: $U = U_+(1 - a^3/x^3)$, where the x coordinate is measured from the centre of the sphere. Actually, this function satisfies the conditions exactly at point B and approximately at point A (by virtue of the assertion concerning the remoteness of the front) and it can be assumed that the flow separation, the thin boundary layer and the compressibility do not have a significant effect on this distribution. Substituting into (5.3), integrating "in the mean" of the two parts of the resulting equality from a up to the coordinate of the front L and comparing the "averaged" perturbation $\langle H_1 \rangle$ with the terms from the "zeroth approximation" we obtain the following condition for the smallness of the effect of viscosity

$$\langle H_1 \rangle = 3\int_a^L H_1(x)\frac{a^3}{x^4}dx = \frac{12\eta U_+ V_+}{7a} \ll \frac{1}{2}U_+^2 \rightarrow \eta \ll \frac{7aU_+}{24V_+}$$

This estimate is approximate when answering the question as to whether to introduce viscosity into the treatment. For example, $\eta \sim 1$ Pa s in the case of glycerine at a normal temperature and it follows from the estimate that $a \gg 10^{-6}$ m. This estimate is significantly poorer in the case of far less viscous fluids or in taking account of warming up, to which, as is well known, the magnitude of η is exceedingly sensitive.

In taking account of plasticity, the normal stress σ_x must be fixed instead of the pressure. Since an experimental adiabatic curve is used, the relations on the front remain the same as before. Behind the front, according to the asymptotic approach [2], we assume that plasticity gives a correction to the hydrodynamics which is calculated as the following iteration. As before, in order to obtain the order of magnitude of the correction, it can be assumed that, in the neighbourhood of the stagnation point in the case of a hemisphere, the flow characteristics are close to those which are obtained from the

asymptotic solution of the problem of a non-cavitating viscoplastic flow past a sphere [15]. The correction to the pressure coefficient will the appear as

$$\Delta C_P = \frac{4\tau_d V_-}{\sqrt{3}U_-^2}\left(4\ln\frac{\sqrt{3}\mu}{\tau_d}+1\right) \tag{5.5}$$

where τ_d is the dynamic yield stress (according to von Mises) and μ is the shear modulus.

Judging from experiments [1], the yield stress τ_d, which corresponds to the state of the medium behind the front, is a parameter of the process which is much less than the dynamic elastic limit calculated using measurements of the amplitude of an elastic forerunner and much closer in magnitude to the static yield stress, exceeding it by a factor of 1.5–3. It is clear from the structure of (5.5) that the correction rapidly decreases as the flow velocity increases. In the case of the clay, the preliminary values of the parameters are: $\tau \cong 3 \times 10^6$ Pa, $\mu/\tau_d \cong 10^2$ and, when $M > 1.2$, ΔC_P will be $<10^{-2}$.

In the case of phase transitions, which are revealed, in particular, by breaks in the shock adiabatic curves, the D–u relation is partially piecewise-linear and the calculation then becomes slightly more difficult.

I wish to thank L. B. Al'tshuller for useful information.

This research was carried out with financial support from the Russian Foundation for Basic Research (16530) and the International Science Foundation (MN 1000).

REFERENCES

1. BIVIN Yu. K., KOLESNIKOV V. A and FLITMAN L. M., Determination of the mechanical properties of a medium by the method of dynamic penetration. *Izv. Akad. Nauk SSSR, MTT* 5, 181–185, 1982.
2. FLITMAN L. M., Subsonic axially symmetric elastoplastic flow around slender tapered solids of revolution. *Izv. Akad. Nauk SSSR, MTT* 4, 155–164, 1991.
3. SIMONOV I. V., Cavitational penetration of minimal drag bodies into a rigid medium. *Prikl. Mat. Mekh.* **57**, 6, 110–119, 1993.
4. BIVIN Yu. K. and SIMONOV I. V., Estimates of the depths of penetration of rigid bodies into soil media at supersonic entry velocities. *Dokl. Ross. Akad. Nauk* **328**, 4, 447–450, 1993.
5. NIKOLAYEVSKII V. N. (Ed.), *High Velocity Impact Phenomena*. Mir, Moscow, 1973.
6. AL'TSHULLER L. V. and PAVLOVSKII M. N., Investigation of clay and an argillaceous schist under powerful dynamic actions. *Zh. Prikl. Mat. Mekh. Tekh. Fiz.* 1, 171–176, 1971.
7. NIKOLAYEVSKII V. N., *Mechanics of Porous and Cracked Media*. Nedra, Moscow, 1984.
8. DUBROVSKII I. M., YEGOROV B. V. and RYABOSHAPKA K. P., *Handbook of Physics*. Naukova Dumka, Kiev, 1986.
9. LAGUNOV V. A. and STEPANOV V. A., Measurements of the dynamic compressibility of sand at high pressures. *Zh. Prikl. Mekh. Tekh. Fiz.* 1, 88–96, 1963.
10. TRUNIN R. F., SIMAKOV G. V. and PODURETS M. A., Compression of porous quartz by strong shock waves. *Izv. Akad. Nauk SSSR, Fizika Zemli* 2, 33–39, 1971.
11. KUZNETSOV N. M., Equation of state and the heat capacity of water over a wide range of thermodynamic parameters. *Zh. Prikl. Mekh. Tekh. Fiz.* 1, 112–120, 1961.
12. AL'YEV G. A., Cavitating transonic flow of water around a circular cone. *Izv. Akd. Nauk SSSR, MZhG* 2, 152–154, 1983.
13. BAKHARAKH S. M., VINOKUROV O. A., GORBENKO G. B. *et al.*, Numerical investigation of the process of penetration at a constant velocity into a compressible fluid of undeformable cylinders. *Zh. Prikl. Mekh. Tekh. Fiz.* 5, 150–155, 1989.
14. BATCHELOR G., *Introduction to Fluid Dynamics*. Mir, Moscow, 1973.
15. FLITMAN L. M., Non-cavitating high velocity elastoplastic flow around a blunt body. *Prikl. Mat. Mekh.* **54**, 4, 642–651, 1990.
16. GRIGORYAN S. S., Approximate solution of the problem of the penetration of a body into soil. *Izv. Ross. Akad. Nauk, MZhG* 4, 18–24, 1993.
17. HILL R., Cavitation and the influence of headshape in attack of thick targets by non-deforming projectiles. *J. Mech. Phys. Solids* **28**, 249–263, 1980.

Translated by E.L.S.